Atmos. Chem. Phys., 11, 4861–4872, 2011
www.atmos-chem-phys.net/11/4861/2011/
doi:10.5194/acp-11-4861-2011

Atmospheric Chemistry and Physics

Measurement from sun-synchronous orbit of a reaction rate controlling the diurnal NO_x cycle in the stratosphere

J. C. Walker and A. Dudhia

Atmospheric, Oceanic and Planetary Physics, Clarendon Laboratory, University of Oxford, Oxford, OX1 3PU, UK

Received: 23 August 2010 – Published in Atmos. Chem. Phys. Discuss.: 21 October 2010
Revised: 25 April 2011 – Accepted: 29 April 2011 – Published: 24 May 2011

Abstract. A reaction rate associated with the nighttime formation of an important diurnally varying species, N_2O_5, is determined from MIPAS-ENVISAT. During the day, photolysis of N_2O_5 in the stratosphere contributes to nitrogen-catalysed ozone destruction. However, at night concentrations of N_2O_5 increase, temporarily sequestering reactive NO_x (NO and NO_2) in a natural cycle which regulates the majority of stratospheric ozone. In this paper, the reaction rate controlling the formation of N_2O_5 is determined from this instrument for the first time. The observed reaction rate is compared to the currently accepted rate determined from laboratory measurements. Good agreement is obtained between the observed and accepted experimental reaction rates within the error bars.

1 Introduction

The importance of N_2O_5 arises mainly from its role as a temporary reservoir for reactive NO_x (NO and NO_2) which catalyse the main ozone-destroying cycles in the stratosphere (Crutzen, 1970). Concentrations of N_2O_5 increase at night and decrease during the day thereby exerting a regulating influence on the rate of ozone destruction throughout the extra-polar stratosphere. The formation of N_2O_5 proceeds at night via the following reactions

$$NO + O_3 \longrightarrow NO_2 + O_2 \quad \text{(R1)}$$

$$NO_2 + O_3 \xrightarrow{k} NO_3 + O_2 \quad \text{(R2)}$$

$$NO_2 + NO_3 + M \longrightarrow N_2O_5 + M \quad \text{(R3)}$$

where M is any molecule. At sunset, almost all NO is converted rapidly into NO_2 via Reaction (R1). The formation of N_2O_5 then proceeds steadily during darkness hours via a two step process involving Reactions (R2) and (R3), where Reaction (R2) is the rate limiting step. The main loss process at night is the thermal decomposition of N_2O_5, which is the reverse of the three-body Reaction in (R3). This process is highly temperature dependent with a time constant of around 3 months at 220 K decreasing to around 30 min at 270 K (Atkinson et al., 2004).

Formation of N_2O_5 is suppressed during the day due to the rapid photolysis of NO_3. After sunrise, concentrations of N_2O_5 decrease steadily during daylight hours due to photolysis by UV radiation in the range 200–400 nm

$$N_2O_5 + h\nu \longrightarrow NO_2 + NO_3 \quad \text{(R4)}$$

where the rate of photolysis depends strongly on the solar zenith angle and the amount of shielding by the overhead ozone column. Loss through thermal decomposition is also ongoing and becomes more important with altitude but is over 10 times slower than the photolytic decay at 40 km and over 100 times slower at 30 km (Connell and Johnston, 1979).

A study by Nevison et al. (1996) assessed the effect of reactions involving $ClONO_2$ and HNO_3 on diurnal variations in NO_x. At night, the reaction

$$ClO + NO_2 + M \longrightarrow ClONO_2 + M \quad \text{(R5)}$$

is important in the lower stratosphere and tends to increase the sunset/sunrise NO_x ratio. The following reaction which occurs on the surface of aerosols

$$N_2O_5 + H_2O \longrightarrow 2HNO_3 \quad \text{(R6)}$$

is also important in the lower stratosphere where the aerosol loading is highest. However, they state that reactions involving $ClONO_2$ and HNO_3 have little influence on the diurnal NO_x cycle above 35 km.

Correspondence to: J. C. Walker
(walker@atm.ox.ac.uk)

Published by Copernicus Publications on behalf of the European Geosciences Union.

2 Previous measurements

The main aim of this study is to determine the reaction rate controlling the nighttime formation of N_2O_5 in Reaction (R2) using measurements from the Michelson Interferometer for Passive Atmospheric Sounding (MIPAS) on board the Environmental Satellite (ENVISAT). While reaction rates can be measured in the laboratory, it is always useful to verify that they apply in the real atmosphere, particularly given that the low temperatures and pressures encountered in the stratosphere are difficult to reproduce in a laboratory environment. Although localised studies have been performed from ground-based or balloon-based experiments, there are few examples of space-based measurements of reaction rates controlling diurnal NO_x chemistry due to the difficulty of following reactions directly from an orbiting platform.

Highly inclined orbits which precess on a short time scale are preferred, as the entire diurnal cycle can be observed over a period of days, which allows the diurnal component of variation to be separated from any longer-term seasonal changes, and for reaction rates to be fitted directly to the observations. The chemistry suite on board the Upper Atmosphere Research Satellite (UARS) launched in 1991 allowed the diurnal NO_x cycle to be observed directly from space from a precessing orbit which sampled the diurnal cycle on the time scale of around one month. Two of the atmospheric chemistry instruments on board: the Cryogenic Limb Array Etalon Spectrometer (CLAES) and the Improved Stratospheric and Mesospheric Sounder (ISAMS), were used to investigate the diurnal NO_x cycle (Kumer et al., 1996; Smith et al., 1996). Although these measurements were able to confirm theoretical predictions about the qualitative behaviour of the diurnal NO_x cycle, the accuracy of the data did not allow for confirmation of the value of key parameters controlling its behaviour, in particular the reaction rates controlling the nighttime formation of N_2O_5 and the rate of photolysis of N_2O_5. This was due in part to the eruption of Mount Pinatubo in 1991 which led to the formation of large amounts of sulphate aerosol in the stratosphere. This added to the inherent problem of distinguishing the weak, continuum-like signal of N_2O_5 from unknown spectral offsets, and so hindered attempts to fully characterise gaseous phase NO_x chemistry.

The earliest space-based tests of the parameters used to model the diurnal NO_x cycle were performed by Allen et al. (1990) using a limited number of solar occulation measurements during the Atmospheric Trace Molecule Spectroscopy (ATMOS) experiment on board Spacelab 3. This was a shuttle-based experiment which used measurements of the NO/NO_2 ratio at sunrise and sunset to evaluate the temperature dependent rate of Reaction (R2). They concluded that the reaction rate was properly parameterised in current models.

Stratospheric NO_x chemistry was also tested from space more recently using the Global Ozone Monitoring by Occultation of Stars (GOMOS) instrument on board ENVISAT considering 465 stellar occultations (Marchand et al., 2004). The GOMOS measurements of NO_2 and ozone were assimilated into a photochemical scheme to provide an estimate of the NO_3 concentration which was compared against the measured value for that species. This provided a quantitative test of the understanding of stratospheric NO_x chemistry as well as a test for the self-consistency of the GOMOS measurements. Differences between the analysed and measured NO_3 were found to be small which suggested that the nighttime NO_x chemistry was well characterised.

In another study using the GOMOS instrument, stratospheric temperature was retrieved using measurements of NO_3 and ozone using knowledge of the temperature dependency of Reaction (R2) (Marchand et al., 2007). Comparisons of the retrieved temperature against ECMWF temperatures suggested that the rate of Reaction (R2) agreed with the accepted reaction rate determined from laboratory measurements.

The High Resolution Dynamics Limb Sounder (HIRDLS) on board Aura was originally intended to measure N_2O_5. However, due to calibration issues arising from a dislodged piece of Kapton insulation, which almost completely blocked the field-of-view, N_2O_5 has not yet been used extensively from this instrument.

The Atmospheric Chemistry Experiment (ACE) Fourier Transform Spectrometer (FTS) on board SCISAT-1, which works by solar occultation, is able to measure NO_x from space. To our knowledge, however, these measurements have so far not been used to determine reaction rates associated with the diurnal NO_x cycle.

In this paper, the rate of Reaction (R2) which regulates the bulk of ozone destruction in the stratosphere (Allen et al., 1990) is determined using data from MIPAS-ENVISAT. The reaction rate as observed using MIPAS is compared against the accepted rate determined from laboratory measurements. The characteristics of the MIPAS instrument are described in Sect. 3, and the retrievals of chemical species required to determine the reaction rate are described in Sect. 4. In Sect. 5, the currently accepted laboratory measurements are introduced and a method to determine the reaction rate using MIPAS is described. The temperature dependence of the observed reaction rate is determined in Sect. 6.2. Then in Sect. 6.3, the seasonal effects on the observed reaction rate are examined.

3 MIPAS-ENVISAT

MIPAS-ENVISAT is a high spectral resolution limb-viewing Fourier transform spectrometer, measuring thermal emission in five spectral bands (A 685–970 cm^{-1}; AB 1020–1170 cm^{-1}; B 1215–1500 cm^{-1}; C 1570–1750 cm^{-1}; D 1820–2410 cm^{-1}). The instrument sits in a sun-synchronous polar orbit and provides global coverage each day. From July 2002 until March 2004 the instrument operated in its

full spectral resolution mode ($0.0250\,cm^{-1}$ spectral sampling) with scans spaced by approximately 5° in latitude each consisting of 17 spectra acquired at altitudes between 6 and 68 km. In late March 2004, problems developed in the interferometer drive mechanism and the instrument was switched off for several months. Several new measurement modes were introduced in January 2005 using a reduced spectral resolution and finer vertical measurement grid. In this study, the analysis has been limited to the full resolution dataset in order to avoid complications due to systematic differences between the various measurement modes that are not fully characterised.

4 Retrievals

Retrievals of N_2O_5, NO_2, ozone and temperature were performed using the MIPAS Orbital Retrieval using Sequential Estimation (MORSE) algorithm (Dudhia, 2008) with MIPAS version 4.61/4.62 full resolution level 1b spectra. Spectroscopic data was derived from the HITRAN spectroscopic database (Rothman et al., 1998; Flaud and Carli, 2003) which includes infrared absorption cross-section data for N_2O_5 (Cantrell et al., 1988). The MORSE retrieval uses optimal estimation (Rodgers, 2000) which includes prior information about the expected profile to constrain the retrieved values. The a priori volume mixing ratio (VMR) profiles were derived from a climatological database and do not include the diurnal variation (Remedios et al., 2007). To ensure that the influence of the a priori estimate was acceptably small, retrieved values with an a priori contribution of greater than 50 % were removed from the analysis. Cloud contaminated spectra were identified using the method by Spang et al. (2004) and were discarded. In the retrieval of each target species, a sequential retrieval of interfering species VMR was performed beforehand for each spectrum in order of greatest contribution to radiance. The spectral regions used to retrieve each target species in a given altitude range are shown in Fig. 1. These regions were chosen to minimise random and systematic errors in the retrieved state as described in Dudhia et al. (2002).

Retrievals of N_2O_5 were performed using the ν_{12} band centred on $1246\,cm^{-1}$. The retrieval of N_2O_5 is complicated by its weak, continuum-like spectral signature which is difficult to distinguish from the spectrally flat background continuum arising from unknown contributions due to cloud and aerosol, unmodelled contributions from interfering species, and uncertainties in instrumental effects. A higher cloud index of 4 was therefore used to minimise the effect of the background continuum as much as possible. To separate the N_2O_5 signal from the remaining background continuum, spectral points were included on the edge of the N_2O_5 ν_{12} band where radiance can mostly be attributed to the background continuum rather than N_2O_5. A joint retrieval of N_2O_5 and a continuum term was then performed at each tangent altitude helping to separate the two contributions. A similar approach was adopted in the retrieval of N_2O_5 from MIPAS-ENVISAT by Mengistu Tsidu et al. (2004).

The total error budget in the mid-stratosphere for tangent altitudes of 33, 36, and 39 km was calculated for temperature, NO_2, N_2O_5, and ozone considering a single profile for a standard atmosphere. The random error was calculated considering the propagation of instrument noise through the retrieval. The systematic error was computed considering the sum of estimated 1σ errors on parameters subject to uncertainty within the retrieval including temperature and pressure retrieval errors, variability in interfering species, instrument calibration uncertainties, the horizontal temperature gradient, and uncertainties in the spectroscopic database. The total error was then computed by combining the random and systematic components in quadrature. Details of these calculations can be found in Dudhia et al. (2002). The total error budget in this altitude range was found to be 1.7–1.9 K for temperature, 7.2–13.9 % for NO_2, 7.5–17.1 % for N_2O_5, and 9.0–10.0 % for ozone. Significant averaging of the data is performed in this study and so the random component can be ignored leaving the systematic component which was found to account for 0.9–1.2 K for temperature, 5.4–8.0 % for NO_2, 4.4–7.4 % for N_2O_5, and 4.4–7.0 % for ozone.

5 Determination of the reaction rate

5.1 Laboratory measurements

The recommended rate of Reaction (R2) used in stratospheric chemical modelling is calculated using the Arrhenius expression for 2nd order reactions given by

$$k(T) = A\,\exp\left(\frac{-E}{R\,T}\right) \tag{1}$$

where k is in units of $cm^3\,molecule^{-1}\,s^{-1}$, A is the Arrhenius factor, T is kinetic temperature, E is the activation energy and R is the molar gas constant. As summarised in the JPL recommendations in DeMore et al. (1997), the preferred values for the Arrhenius factor ($A = 1.2\times10^{-13}\,cm^3\,molecule^{-1}\,s^{-1}$) and temperature coefficient ($E/R \pm (\Delta E/R) = 2450 \pm 150\,K$) are derived from a least squares fit of results from laboratory studies by Davis et al. (1974), Graham and Johnston (1974), and Huie and Herron (1974), which were found to be in excellent agreement in the temperature range examined between 231 and 362 K, as well as with room temperature measurements by Cox and Coker (1983), see Table 1. The reaction rate derived from these studies and cited in DeMore et al. (1997) is recommended for use at temperatures between 200–300 K. However, the reaction rate has not yet been verified at temperatures below around 230 K which are commonly observed in the lower stratosphere. In DeMore et al. (1997), the error on

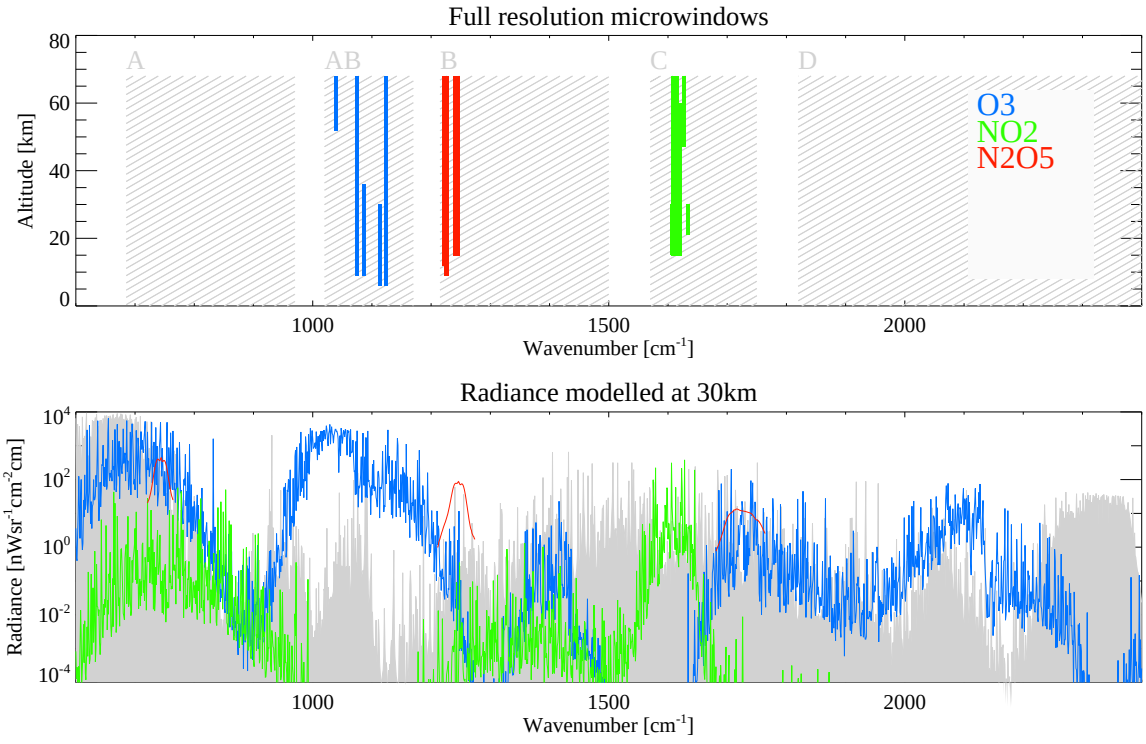

Fig. 1. Top panel shows the spectral regions used to retrieve N_2O_5 in red, NO_2 in green and ozone in blue. Grey shaded area in the top panel shows the spectral coverage of MIPAS-ENVISAT. Bottom panel shows the contribution to modelled limb radiance at 30 km for each species for a standard atmosphere. Contribution of other molecules (mainly water vapour and CO_2) shown in grey.

the Arrhenius estimate of the reaction rate due to experimental uncertainties may be calculated as

$$f(T) = f(298)\exp\left(\frac{\Delta E}{R}\left(\frac{1}{T}-\frac{1}{298}\right)\right) \quad (2)$$

where $f(298) = 1.15$ and $f(T)$ is a multiplicative factor which gives the upper and lower bounds of k corresponding approximately to one standard deviation.

5.2 Observed values

The aim of this study is to compare the recommended value of the reaction rate given by the Arrhenius equation against an estimate derived from MIPAS-ENVISAT measurements which does not depend on any of the laboratory-determined parameters used in Eq. (1). This provides useful evidence in support of the laboratory work, as well as providing an indication of how well the recommended expression performs at the very low temperatures in the stratosphere which are difficult to reproduce in the laboratory. The reaction rate (in units of $\mathrm{ppmv}^{-1}\,\mathrm{h}^{-1}$, where ppmv is the volume mixing ratio in parts per million) may be derived from MIPAS-ENVISAT measurements using the following expression

$$k_{\mathrm{obs}} = \frac{1}{2[\mathrm{O_3}]t}\ln\left(\frac{2\Delta[\mathrm{N_2O_5}]}{[\mathrm{NO_2}]}+1\right); \quad (3)$$
$$\Delta[\mathrm{N_2O_5}] = [\mathrm{N_2O_5}] - [\mathrm{N_2O_5}]_{\mathrm{set}}$$

where t is the number of hours since sunset of the observation, $[N_2O_5]$, $[NO_2]$ and $[O_3]$ are the observed nighttime volume mixing ratios of those species in ppmv, and $[N_2O_5]_{\mathrm{set}}$ is the sunset concentration (Toumi et al., 1991). This estimate will be denoted k_{obs} to distinguish it from the standard value of the reaction rate k determined using the Arrhenius equation. This approach has the advantage of providing an estimate of the reaction rate for a single set of measurements without the need to track diurnal changes, which is suited to the limited sampling provided in a sun-synchronous orbit. All quantities in Eq. (3) can be measured directly using MIPAS except the sunset concentration of N_2O_5. The concentration of N_2O_5 remaining at sunset is usually negligible except at high latitudes in the winter months, where the short days and high solar zenith angle result in weak photolysis of N_2O_5. In these situations, the N_2O_5 at sunset may be calculated using the measured daytime concentration of N_2O_5 with photolysis rates derived from the Tropospheric Ultraviolet and Visible Radiation Model (TUV) (Madronich, 2006) to extrapolate to the sunset value. At lower latitudes and in summertime at high latitudes, the residual at sunset is very close to zero and can be neglected.

The main assumptions behind the derivation of Eq. (3) have already been investigated in some detail by Nevison et al. (1996) through comparisons against photochemical models. These assumptions are that the concentration of

Table 1. Table summarising main laboratory measurements of Reaction (R2) given by $NO_2+O_3 \xrightarrow{k} NO_3+O_2$ adapted from Atkinson et al. (2004). The recommended value of k in DeMore et al. (1997) is based on a least squares fit analysis of the data presented in the first three studies listed below.

k/cm^3 molecule^{-1} s^{-1}	Temp/K	Reference
$9.76\times10^{-14}\exp[-(2427\pm140)/T]$	260–343	Davis et al. (1974)
$1.34\times10^{-13}\exp[-(2466\pm30)/T]$	231–298	Graham and Johnston (1974)
$1.57\times10^{-13}\exp[-(2509\pm76)/T]$	259–362	Huie and Herron (1974)
$(3.78\pm0.07)\times10^{-17}$	297	Cox and Coker (1983)
$(3.45\pm0.12)\times10^{-17}$	296	

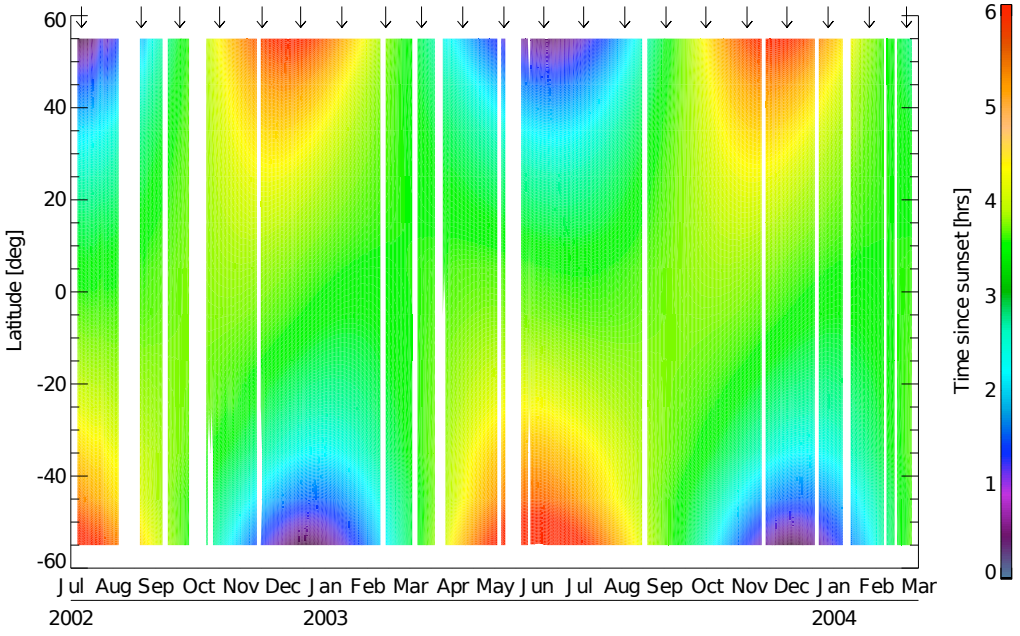

Fig. 2. Seasonal variation in time since sunset of MIPAS-ENVISAT nighttime observations. Arrows indicate sample days used to compute the reaction rate (9 July 2002, 23 August 2002, 21 September 2002, 21 October 2002, 22 November 2002, 21 December 2002, 21 January 2003, 23 February 2003, 22 March 2003, 22 April 2003, 23 May 2003, 22 June 2003, 22 July 2003, 22 August 2003, 22 September 2003, 22 October 2003, 22 November 2003, 22 December 2003, 22 January 2004, 22 February 2004, 22 March 2004). Red colours indicate summertime observations furthest from sunset. Blue colours indicate wintertime observations closest to sunset. White areas indicate where data was unavailable.

ozone remains constant over the course of the night, that thermal decomposition of N_2O_5 is negligible, that concentrations of NO_3 are in a steady state throughout the night, and that losses of NO_2 to the longer-lived reservoirs HNO_3 and $ClONO_2$ can be ignored. Using a 1-D model of reactive nitrogen chemistry with 12 relevant reactions, Nevison et al. (1996) concluded that thermal decomposition of N_2O_5 was not significant below 40 km. This is confirmed by inspection of Figs. 5 and 6, which show the time constant for the thermal decomposition of N_2O_5 and the observed stratospheric temperature respectively. The time constant is much longer than the diurnal time scale in most cases and so can reasonably be ignored. In addition, loss of NO_x to the longer-lived reservoirs HNO_3 and $ClONO_2$ can also be ignored in many circumstances. In the same study by Nevison et al. (1996), comparisons against the 2-D chemical-radiative-dynamical model by Garcia and Solomon (1994) indicated that the formation of HNO_3 and $ClONO_2$ over the course of the night was only significant below around 35 km. Overall, their study suggests that k_{obs} can be used to provide an estimate of the reaction rate in the mid-stratosphere where thermal decomposition of N_2O_5, loss of NO_x to $ClONO_2$, and heterogeneous loss to HNO_3 can be ignored. Therefore, in this study the determination of the reaction rate using Eq. (3) is limited to mid-stratospheric measurements at nominal tangent altitudes of 33, 36 and 39 km.

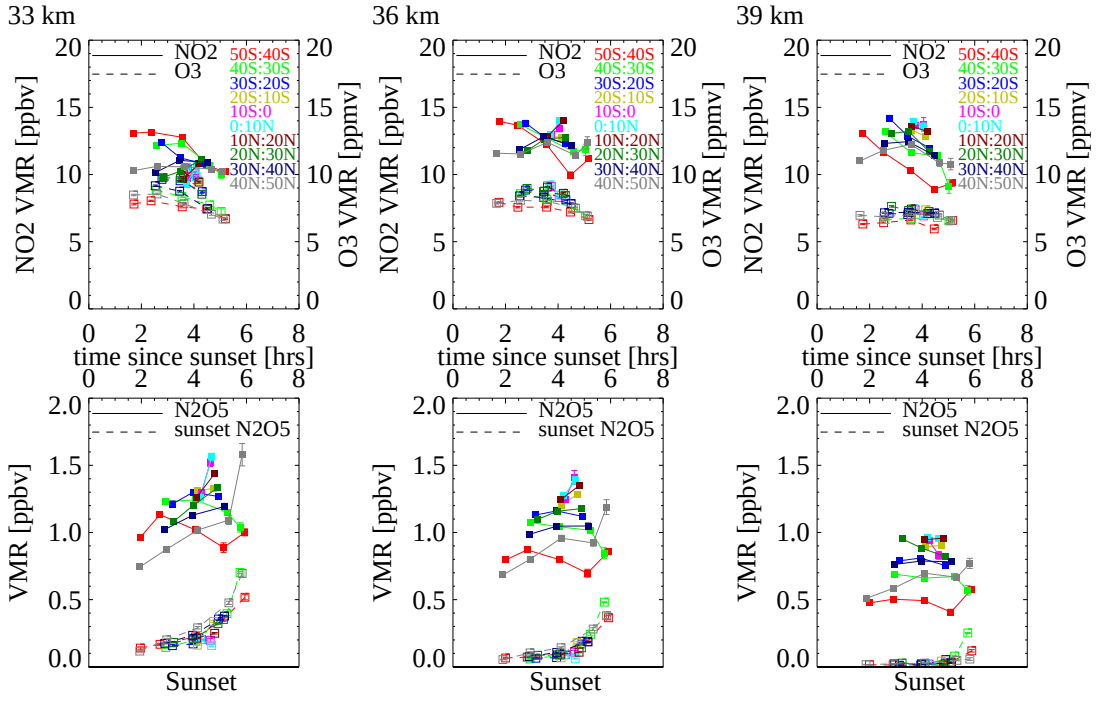

Fig. 3. Top panel shows the measured nighttime concentrations of NO_2 and ozone binned by hour since sunset in 10° latitude bands where 50–40° S is shown in red, 40–30° S in light green, 30–20° S in dark blue, 20–10° S in yellow, 10–0° S in pink, 0–10° N in light blue, 10–20° N in maroon, 20–30° N in dark green, 30–40° N in navy blue, and 40–50° N in grey. In the bottom panel, latitude bands are coloured as in top panel. The filled squares show the measured nighttime concentrations of N_2O_5 at the given time since sunset (upper axis) for the given bin. The empty squares show the N_2O_5 concentration at sunset (lower axis) modelled using the TUV for the given latitude bin. Error bars indicate error in mean.

6 Results

Although an estimate of the reaction rate k_{obs} can be obtained using a single set of measurements using Eq. (3), including many measurements at different times of year and at different latitudes allows a better comparison of k_{obs} against the accepted reaction rate k. In this way a wide range of stratospheric temperatures may be examined in the calculation of the reaction rate. In a sun-synchronous orbit, higher latitudes have a greater spread in the time since sunset of nighttime measurements over the changing seasons, with summertime measurements that are close to sunset and wintertime measurements that are much later at night, as shown in Fig. 2. By examining measurements obtained in all seasons at different points during the diurnal cycle, it is possible to separate situations where the assumptions behind Eq. (3) are thought to be good from those situations where the estimates may be less reliable.

6.1 Overview of data

The analysis of the reaction rate is performed using zonally averaged data which assumes that the aspects controlling the diurnal cycle such as stratospheric temperature and rate of photolytic decay of N_2O_5 have much stronger latitudinal than longitudinal dependencies, which is reasonable at extra-polar latitudes in the stratosphere. Figure 3 shows the nighttime retrieved values of N_2O_5, NO_2, and ozone at 33, 36 and 39 km binned in 10° latitude bands by time since sunset of the observation grouped by hour. The estimated sunset concentrations of N_2O_5 corresponding to the measurements in each bin are also shown. These sunset values were calculated using the daytime measurements of N_2O_5 in Fig. 4 with photolysis rates derived from the TUV considering the measured overhead ozone column to extrapolate the expected concentration of N_2O_5 remaining at sunset. Figure 3 shows the nighttime evolution of the components of NO_x across the seasons, with summertime measurements corresponding to observations that are close to sunset and wintertime measurements corresponding to observations that are later at night. It is not possible to attempt to fit the reaction rate controlling the formation of N_2O_5 to the data points directly due to the underlying seasonal variations, in particular temperature, that are unaccounted for.

6.2 Temperature dependence of the reaction rate

Instead, in Figs. 7–9, the temperature dependence of the reaction rate k computed using the Arrhenius expression in Eq. (1) is examined in comparison with the MIPAS observations of the reaction rate k_{obs} calculated using Eq. (3) in 5 K temperature bins allowing for a possible non-negligible

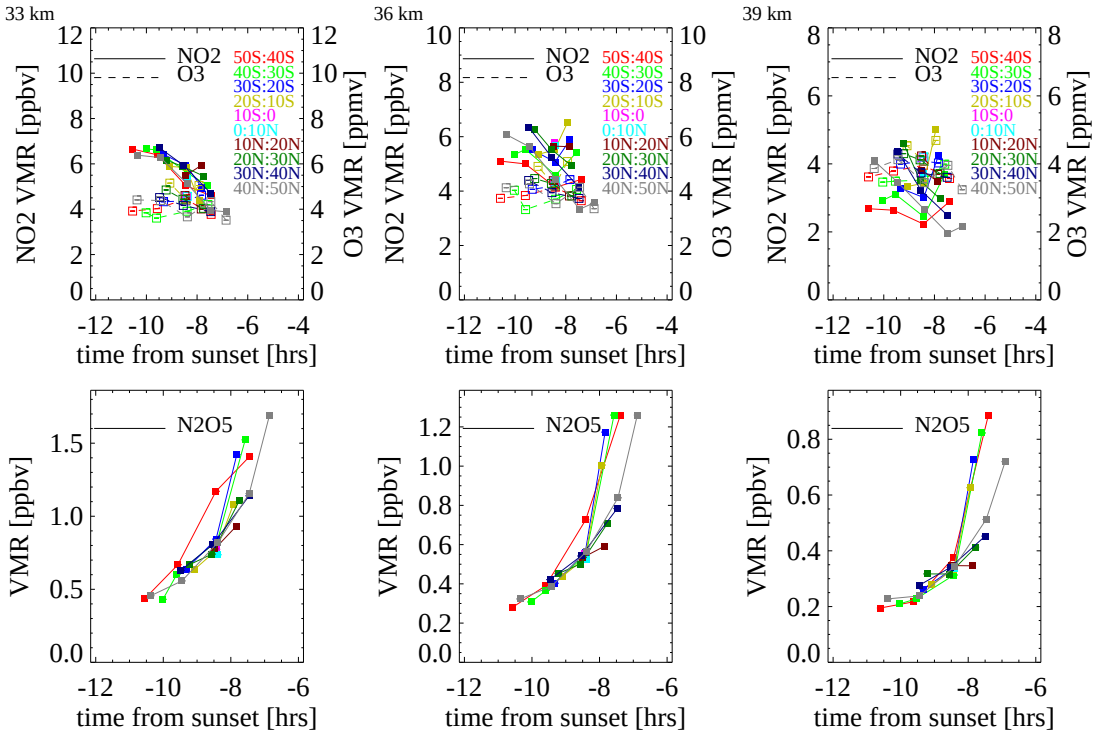

Fig. 4. Top panel shows the measured daytime concentrations of NO_2 and ozone binned by hour from sunset in 10° latitude bands where 50–40° S is shown in red, 40–30° S in light green, 30–20° S in dark blue, 20–10° S in yellow, 10–0° S in pink, 0–10° N in light blue, 10–20° N in maroon, 20–30° N in dark green, 30–40° N in navy blue, and 40–50° N in grey. Bottom panel shows the measured daytime concentrations of N_2O_5 binned in the same way. These measurements were used to initialise the photolysis calculations to calculate the sunset values of N_2O_5 using the TUV. The calculated sunset values are shown in the bottom panel of Fig. 3. Error bars indicate error in mean.

sunset N_2O_5 concentration. The k_{obs} estimates follow the expected exponential temperature dependence well, and there is qualitative agreement with the JPL recommendation within the estimated error in almost all cases examined. A deviation of k_{obs} below k is seen at all altitudes for temperatures above 250 K, as this is where thermal decomposition of N_2O_5, which was neglected in the formulation of Eq. (3), becomes significant in comparison to the time elapsed since sunset of the observation. Ignoring thermal decomposition of N_2O_5 means that the anticipated increase in nighttime N_2O_5 is faster that that observed, and so a lower k_{obs} is ascribed to the measurements. However, there appears to be good agreement at all altitudes for temperatures between 220 and 250 K. At low temperatures, there is agreement down to temperatures in the 210–215 K bin at 33 km and down to temperatures in the 205–210 K bin at 36 km, providing observational evidence in support of the reaction rate at the low end of the recommended range in DeMore et al. (1997). The comparison is made more quantitative by fitting an exponential relationship to the MIPAS observations of the reaction rate. The Arrhenius factor (A) and temperature coefficient (E/R) were determined by a best fit to the data in the least squares sense. Observations of the reaction rate at temperatures above 250 K were not included in the fit because of the effects of thermal decomposition that were not

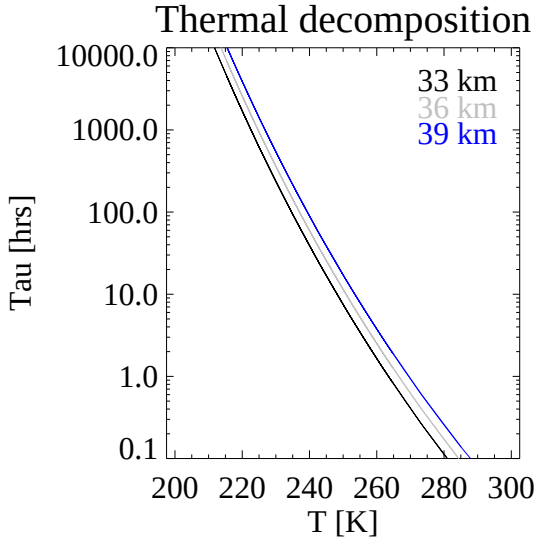

Fig. 5. Time constant of thermal decomposition of N_2O_5 (reverse of Reaction R3) versus temperature at 33 (shown in black), 36 (shown in grey) and 39 km (shown in blue) altitude calculated considering suitable climatological molecular densities at each altitude.

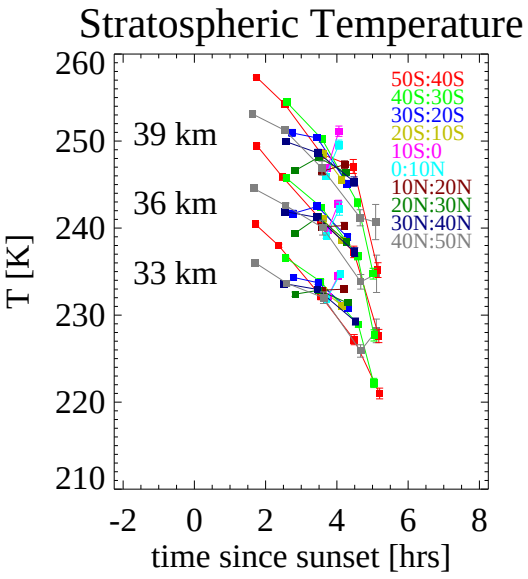

Fig. 6. Stratospheric temperature observed by MIPAS at 33, 36 and 39 km binned by hour since sunset in 10° latitude bands where 50–40° S is shown in red, 40–30° S in light green, 30–20° S in dark blue, 20–10° S in yellow, 10–0° S in pink, 0–10° N in light blue, 10–20° N in maroon, 20–30° N in dark green, 30–40° N in navy blue, and 40–50° N in grey. Error bars indicate error in mean.

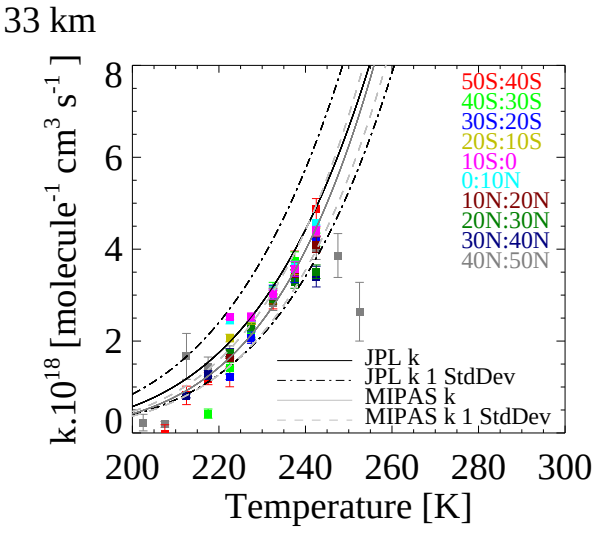

Fig. 7. Temperature dependence of reaction rate at 33 km using $k_{\mathrm{obs}} = \frac{1}{2[O_3]t}\ln\left(\frac{2\Delta[N_2O_5]}{[NO_2]}+1\right)$ in Eq. (3) assuming possible non-negligible $[N_2O_5]$ at sunset binned in 5 K temperature increments in 10° latitude bands where 50–40° S is shown in red, 40–30° S in light green, 30–20° S in dark blue, 20–10° S in yellow, 10–0° S in pink, 0–10° N in light blue, 10–20° N in maroon, 20–30° N in dark green, 30–40° N in navy blue, and 40–50° N in grey. The solid grey line shows the best fit to this data and the dashed grey line shows the estimated 1 σ error of the fit. This estimate is compared against the temperature dependence computed using the Arrhenius expression $k(T) = A\ \exp\left(\frac{-E}{RT}\right)$ in Eq. (1) which is shown as a solid black line with the estimated 1 σ error indicated as a dot-dashed black line.

accounted for. The best fit curves are shown in Figs. 7–9. Within the temperature range examined the observed reaction rate agrees with the JPL recommendation within the estimated 1σ error. The fitted Arrhenius parameters from observations at 33, 36, and 39 km are listed in Table 2. The reaction rate considering the best fit parameters at 245 K is also shown. The 1σ errors for the reaction rate were computed assuming the errors in the fitted parameters A and E/R could be combined linearly. The overall best fit estimate of k at 245 K computed combining all estimates is then given by $(5.3 \pm 0.6) \times 10^{-18}$ cm^3 molecule^{-1} s^{-1}. The value of k at 245 K derived from the JPL recommendation is $(5.4^{+1.5}_{-1.3}) \times 10^{-18}$ cm^3 molecule^{-1} s^{-1}, where the estimated 1σ errors are computed using Eq. (2). The observational estimate of the reaction rate is therefore in agreement with the JPL recommendation at stratospheric temperatures within the errors.

6.3 The reaction rate by season

In Figs. 10–12, the reaction rate k_{obs} at 33, 36, and 39 km is presented grouped by latitude and time since sunset of the observation, so that measurements taken at the same time of year and latitude are grouped together, allowing situations where the underlying assumptions in the calculation of k_{obs} are thought to be good to be separated from those situations where the assumption may be less reliable. The observed temperature corresponding to each estimate of the reaction rate is shown in Fig. 6.

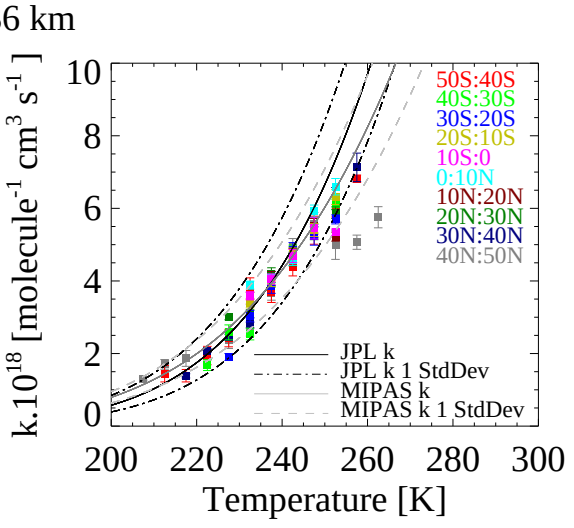

Fig. 8. As in Fig. 7 but at 36 km.

As expected, the reaction rate is higher in the warmer summertime atmosphere, corresponding to measurements a long time after sunset and conversely, the reaction rate is slower in the colder wintertime atmosphere. To aid the analysis of

Table 2. Table summarising the MIPAS observations of k in comparison to the JPL recommendation for Reaction R2 ($NO_2 + O_3 \xrightarrow{k} NO_3 + O_2$). The values for the pre-exponential parameter (A) and the activation temperature (E/R) are derived from the data shown in Figs. 7–9 at 33, 36 and 39 km. The value of the reaction rate at 245 K is shown for all cases.

		A/cm^3 molecule^{-1} s^{-1}	(E/R)/K	Temp/K	k/cm^3 molecule^{-1} s^{-1} at 245 K
JPL		1.2×10^{-13}	2450 ± 150	200–300	$(5.4^{+1.5}_{-1.3}) \times 10^{-18}$
MIPAS	33 km	$(3.2 \pm 0.3) \times 10^{-13}$	2708 ± 18	200–250	$(5.0 \pm 0.5) \times 10^{-18}$
	36 km	$(20.1 \pm 2.6) \times 10^{-15}$	2028 ± 30	205–250	$(5.1 \pm 0.9) \times 10^{-18}$
	39 km	$(14.3 \pm 2.4) \times 10^{-15}$	1914 ± 38	210–250	$(5.8 \pm 1.3) \times 10^{-18}$

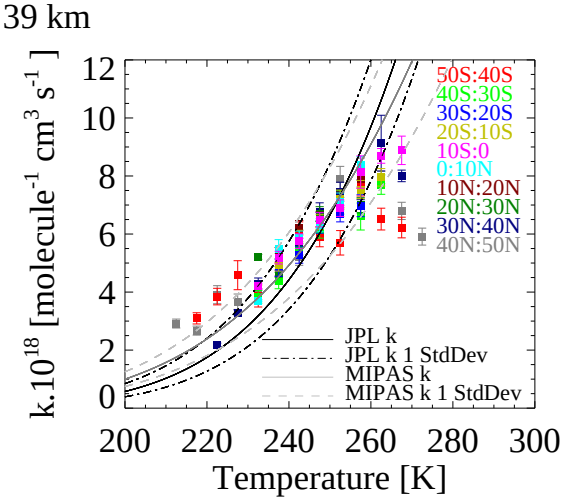

Fig. 9. As in Fig. 7 but at 39 km.

the various biases between k_{obs} and k, estimates of k_{obs} are scaled to a temperature of 245 K using the Arrhenius equation

$$k'_{obs} = k_{obs} \exp\left(\frac{E}{R}\left(\frac{1}{T} - \frac{1}{245}\right)\right) \quad (4)$$

where T is the measured stratospheric temperature.

There is good agreement between k'_{obs} and the JPL recommendation for the reaction rate at 245 K in Figs. 10–12. The discrepancies at long times since sunset and small times since sunset between the observed and laboratory reaction rates can mostly be explained by considering the various assumptions behind the observational estimates. The results accounting for a possible non-negligible sunset N_2O_5 concentration are shown in the middle panel of Figs. 10–12. Results assuming that N_2O_5 is completely photolysed by nightfall and that the sunset concentration is zero are shown in the bottom panel of each figure. It is interesting to note that where the sunset concentration of N_2O_5 is assumed to be zero, there is slightly better agreement between the observed reaction rate and the recommended rate in the tropical latitude bands and in the spring and autumn high latitude estimates at 2–4 h from sunset. In these cases, the sunset concentration is expected to be negligible. Introducing the photolysis calculations results in a slight downwards trend in the reaction rate at 33 and 36 km, which might point to an underestimation of the photolytic decay of N_2O_5 at these altitudes. It has been noted in the past that the photolysis rates are a source of uncertainty and are still not well tested. Photolysis rates which are too fast due to possible problems with the absorption cross-sections or quantum yields were suggested as a possible reason for overestimation of the diurnal NO_x cycle by the ECHAM5/MESSy1 chemistry climate model with respect to the IMK/IAA MIPAS measurements (Brühl et al., 2007). Other authors have concluded that the photolysis of N_2O_5 may be too slow, as was suggested in a study by Allen et al. (1990), which compared ATMOS data with photochemical model results. However, the trend seen here depends on altitude and is less apparent at 39 km, which suggests that it may be due to the assumption that the ozone column remains constant over the course of the day, when in fact concentrations decrease, or that the measured ozone column used in the photolysis calculations is slightly too high. Overall, however, the inclusion of sunset N_2O_5 does generally improve agreement between the observed reaction rate and the recommended rate, removing the upwards trend at long times since sunset. This underlines the difficulty of testing the photolysis rates due to the various geophysical factors affecting the measurement.

The final point to note is the slight upwards trend in observed reaction rates shortly after sunset, especially in the 40–50° N/S latitude bands. This is not related to the photolysis calculations since here sunset concentrations are negligible. Warm stratospheric temperatures mean that the rate of thermal decomposition of N_2O_5 is high. However, the impact of this approximation should still be small since most observations are at temperatures where the thermal decomposition is slow compared to the time elapsed since sunset. For these measurements, the high bias may result from the use of an a priori profile which is higher than the values typically observed under these conditions. As can be seen from Fig. 4, the retrieved values of N_2O_5 are less than 1 ppbv at all altitudes examined for these cases. The retrieval of low

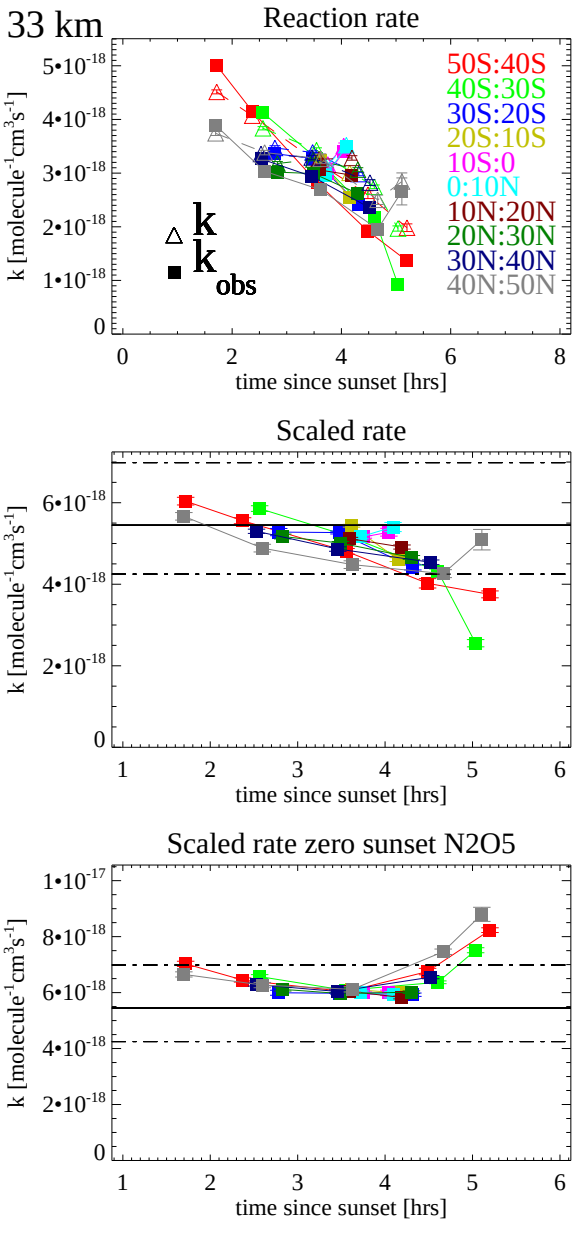

Fig. 10. Seasonal analysis grouped by hour elapsed since sunset where top panel shows k_{obs} and Arrhenius k (computed for observed atmospheric temperature) binned in 10° latitude bands where 50–40° S is shown in red, 40–30° S in light green, 30–20° S in dark blue, 20–10° S in yellow, 10–0° S in pink, 0–10° N in light blue, 10–20° N in maroon, 20–30° N in dark green, 30–40° N in navy blue, and 40–50° N in grey. Middle panel at each altitude shows k_{obs} scaled to the value it would assume at 245 K where the sunset N_2O_5 concentration has been estimated using the TUV. Bottom panel is as in middle panel except sunset N_2O_5 concentrations are assumed to be negligible. The horizontal line in the middle and bottom panels indicates the Arrhenius estimate of the reaction rate at 245 K.

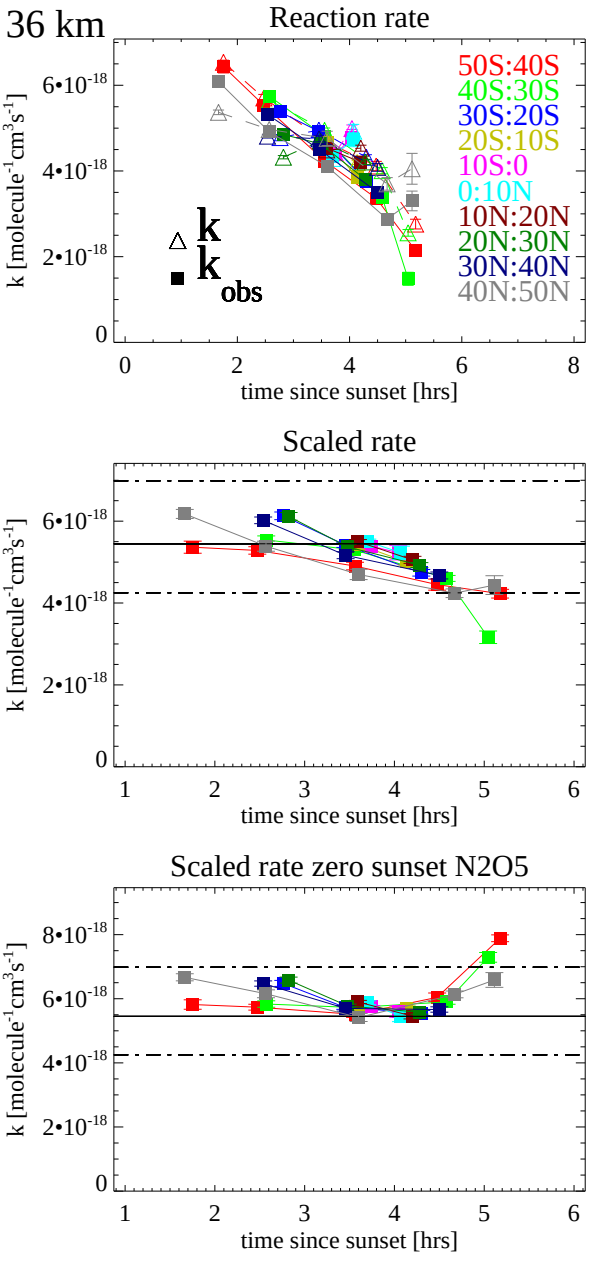

Fig. 11. As in Fig. 10 but at 36 km.

VMR performed in log-space can also lead to a high bias. Although retrieval in log-space ensures that unphysical negative values are not retrieved, for species with very low VMR, the assymetry of the a priori distribution can lead to high biased values even when a suitably large a priori uncertainty is applied. In summary, values of k_{obs} obtained early in the night may be unreliable but highlight the circumstances under which the N_2O_5 retrieval should be treated with caution.

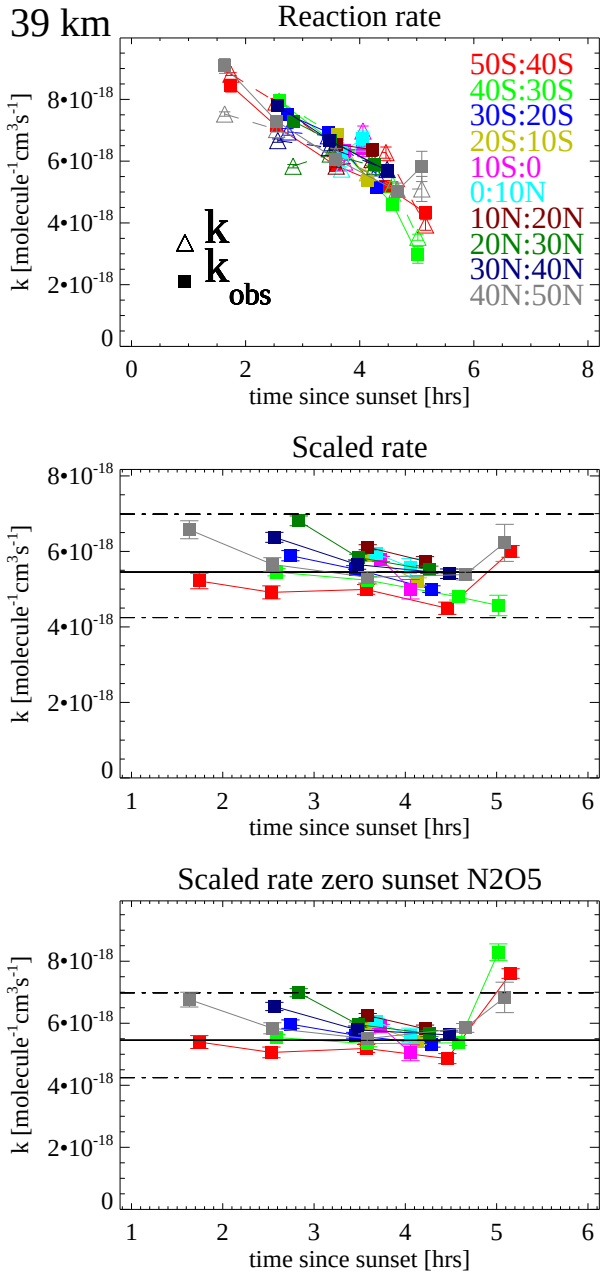

Fig. 12. As in Fig. 10 but at 39 km.

7 Conclusions

The reaction rate controlling the conversion of NO and NO_2 into N_2O_5 at night, which regulates the majority of ozone destruction at extra-polar latitudes, was determined from MIPAS-ENVISAT measurements. Agreement between the observed reaction rate and the recommended reaction rate for use in stratospheric chemical modelling was within the error bars for observations obtained at mid-stratospheric altitudes between 33 and 39 km for temperatures between 205 and 250 K. The results are also in agreement with the reaction rate determined from other space-based studies which suggest that the reaction rate is properly characterised. Overall, these results indicate consistency between the key parameters controlling the diurnal NO_x cycle and the Oxford-based MORSE retrievals of NO_2, N_2O_5, and ozone used in this study.

Acknowledgements. Funded by the Natural Environment Research Council, UK. Thanks to the anonymous reviewers for their comments.

Edited by: W. Lahoz

References

Allen, M., Delitsky, M. L., and Hobbs, P. V.: Stratospheric NO, NO_2, and N_2O_5: A comparison of model results with Spacelab 3 Atmospheric Trace Molecule Spectroscopy (ATMOS) measurements, J. Geophys. Res., 95, 14077–14082, 1990.

Atkinson, R., Baulch, D. L., Cox, R. A., Crowley, J. N., Hampson, R. F., Hynes, R. G., Jenkin, M. E., Rossi, M. J., and Troe, J.: Evaluated kinetic and photochemical data for atmospheric chemistry: Volume I –gas phase reactions of O_x, HO_x, NO_x and SO_x species, Atmos. Chem. Phys., 4, 1461–1738, doi:10.5194/acp-4-1461-2004, 2004.

Brühl, C., Steil, B., Stiller, G., Funke, B., and Jöckel, P.: Nitrogen compounds and ozone in the stratosphere: comparison of MIPAS satellite data with the chemistry climate model ECHAM5/MESSy1, Atmos. Chem. Phys., 7, 5585–5598, doi:10.5194/acp-7-5585-2007, 2007.

Cantrell, C. A., Davidson, J. A., McDaniel, A. H., Shetter, R. E. and Calvert J. G.: Infrared absorption cross sections for N_2O_5, Chem. Phys. Lett., 148, 358–363, 1988.

Connell, P. and Johnston, H.: The thermal dissociation of N_2O_5 in N_2, Geophys. Res. Lett., 6, 553–556, 1979.

Cox, R. A. and Coker, G. B.: Kinetics of the reaction of nitrogen dioxide with ozone, J. Atmos. Chem., 1, 53–63, 1983.

Crutzen, P. J.: The influence of nitrogen oxides on the atmospheric ozone content, Q. J. Roy. Meteor. Soc., 96, 320-325, 1970.

Davis, D. D., Prusazcyk, J., Dwyer, M., and Kim, P.: A stop-flow time-of-flight mass spectrometry kinetics study, Reaction of ozone with nitrogen dioxide and sulfur dioxide, J. Phys. Chem., 78, 1775–1779, 1974.

DeMore, W. B., Sander, S. P., Howard, C. J., Ravishankara, A. R., Golden, D. M., Kolb, C. E., Hampson, R. F., Kurylo, M. J., and Molina, M. J.: Chemical kinetics and photochemical data for use in stratospheric modelling, Tech. rep., JPL, 12, p. 20, 1997.

Dudhia, A.: MIPAS Orbital Retrieval using Sequential Estimation (MORSE), available at: http://www.atm.ox.ac.uk/MORSE/, last access: June 2010.

Dudhia, A., Jay, V., and Rodgers, C. D.: Microwindow selection for high-spectral-resolution sounders, Appl. Optics, 41, 3665–3673, 2002.

Flaud, J. M. and Carli, B.: MIPAS Dedicated Spectroscopic Database, Tech. rep., Institute for Applied Physics "Nello Carrara", available at: http://www.ifac.cnr.it/retrieval/database.html, last access: June 2010.

Garcia, R. R. and Solomon, S.: A new numerical model of the middle atmosphere, 2. Ozone and related species, J. Geophys. Res.-Atmos., 99, 12937–1295151, 1994.

Graham, R. A. and Johnston, H. S.: Kinetics of the gas-phase reaction between ozone and nitrogen dioxide, J. Chem. Phys., 60, 4628–4629, 1974.

Huie, R. E. and Herron, J. T.: The rate constant for the reaction $O_3 + NO_2 \rightarrow O_2 + NO_3$ over the temperature range 259–362 K, Chem. Phys. Lett., 27, 411–414, 1974.

Kumer, J. B., Mergenthaler, J. L., Roche, A. E., Nightingale, R. W., Zele, F., Gille, J. C., Massie, S. T., Bailey, P. L., Connell, P. S., Gunson, M. R., Abrams, M. C., Toon, G. C., Sen, B., Blavier, J.-F., Smith, S. E., and Taylor, F. W.: Comparison of CLAES preliminary N_2O_5 data with correlative data and a model, J. Geophys. Res., 101, 9657–9678, 1996.

Madronich, S.: TUV: Tropospheric Ultraviolet and Visible Radiation Model, Tech. rep., NCAR/ACD, available at: http://cprm.acd.ucar.edu/Models/TUV/, last access: June 2010.

Marchand, M., Bekki, S., Hauchecorne, A., and Bertaux, J.-L.: Validation of the self-consistency of GOMOS NO_3, NO_2 and O_3 data using chemical data assimilation, Geophys. Res. Lett., 31, L10107, doi:10.1029/2004GL019631, 2004.

Marchand, M., Bekki, S., Lefèvre, F., and Hauchecorne, A.: Temperature retrieval from stratospheric O_3 and NO_3 GOMOS data, Geophys. Res. Lett., 34, L24809, doi:10.1029/2007GL030280, 2007.

Mengistu Tsidu, G., von Clarmann, T., Stiller, G. P., Höpfner, M., Fischer, H., Glatthor, N., Grabowski, U., Kellmann, S., Kiefer, M., Linden, M., Milz, M., Steck, T., Wang, D. Y., and Funke, B.: Stratospheric N_2O_5 in the austral spring 2002 as retrieved from limb emission spectra recorded by the Michelson Interferometer for Passive Atmospheric Sounding (MIPAS), J. Geophys. Res., 109, D18301, doi:10.1029/2004JD004856, 2004.

Nevison, C. D., Solomon, S., and Russell, J. M.: Nighttime formation of N_2O_5 inferred from the Halogen Occultation Experiment sunset/sunrise NO_x ratios, J. Geophys. Res., 101, 6741–6748, 1996.

Remedios, J. J., Leigh, R. J., Waterfall, A. M., Moore, D. P., Sembhi, H., Parkes, I., Greenhough, J., Chipperfield, M.P., and Hauglustaine, D.: MIPAS reference atmospheres and comparisons to V4.61/V4.62 MIPAS level 2 geophysical data sets, Atmos. Chem. Phys. Discuss., 7, 9973–10017, doi:10.5194/acpd-7-9973-2007, 2007.

Rodgers, C. D.: Inverse Methods for Atmospheric Sounding, World Scientific, 2000.

Rothman, L. S., Rinsland, C. P., Goldman, A., Massie, S. T., Edwards, D. P., Flaud, J. M., Perrin, A., Camy-Peyret, C., Dana, V., Mandin, J., Y., Schroeder, J., McCann, A., Gamache, R. R., Wattson, R. B., Yoshino, K., Chance, K. V., Jucks, K. W., Brown, L. R., Nemtchinov, V., and Varanasi, P.: The HITRAN Molecular Spectroscopic Database and HAWKS (HITRAN Atmospheric Workstation): 1996 edition, J. Quant. Spectrosc. Ra., 60, 665–710, 1998.

Smith, S. E., Dudhia, A., Morris, P. E., Remedios, J. J., Rodgers, C. D., Taylor, F. W., Kerridge, B. J., Chipperfield, M. P., Kumer, J. B., Roche, A. E., and Gunson, M. R.: Dinitrogen pentoxide measurements from the Improved Stratospheric and Mesospheric Sounder: validation of preliminary results, J. Geophys. Res., 101, 9897–9906, 1996.

Spang, R., Remedios, J. J., and Barkley, M. P.: Colour indices for the detection and differentiation of cloud types in infra-red limb emission spectra, Adv. Space. Res., 33, 1041–1047, 2004.

Toumi, R., Pyle, J. A., Webster, C. R., and May, R. D.: Theoretical interpretation of N_2O_5 measurements, Geophys. Res. Lett., 18, 7, 1213–1216, 1991.